WIRELESS COMMUNICATIONS AND MOBILE COMPUTING
Wirel. Commun. Mob. Comput. (2015)
Published online in Wiley Online Library (wileyonlinelibrary.com). DOI: 10.1002/wcm.2639

RESEARCH ARTICLE

Sliding window energy detection for spectrum sensing under low SNR conditions†

Xin Tian[1], Zhi Tian[2], Erik Blasch[3], Khanh Pham[4], Dan Shen[1] and Genshe Chen[1]*

[1] Intelligent Fusion Technology, Inc., 20271 Goldenrod Lane, Suite 2066, Germantown, MD 20876, USA
[2] Department of Electrical and Computer Engineering, George Mason University, 4400 University Dr, Fairfax, VA 22030, USA
[3] Air Force Research Laboratory, Information Directorate,Rome, NY 13441, USA
[4] Air Force Research Laboratory, Space Vehicles Directorate, Kirtland AFB, NM 87117, USA

ABSTRACT

For spectrum sensing, energy detection has the advantages of low complexity, rapid analysis, and requires no knowledge of the transmission signal, which makes it suitable for a wide range of applications. However, under low signal-to-noise ratio conditions, the required window length (or the time-bandwidth product) for energy detection to achieve a desired detection performance is large. In addition, conventional energy detection assumes that the detection tests are independent, that is, there is no overlap between individual detection tests. These properties significantly reduce the detection speed when energy detection is used for the continuous monitoring over a communication channel for the detection of signal transmission activities. In this paper, we propose a sliding window detection analysis with overlap among multiple tests. Algorithms for effective performance analysis of the proposed sliding window energy detection are proposed. The impact of window length on distribution of detection time is investigated. Simulation results on the proposed sliding window energy detection are also compared with the theoretically predicted and conventional energy detection performance estimates. Copyright © 2015 John Wiley & Sons, Ltd.

KEYWORDS

spectrum sensing; signal transmission detection; sliding window energy detection; correlated detection tests

***Correspondence**

Xin Tian, Intelligent Fusion Technology, Inc., 20271 Goldenrod Lane, Suite 2066, Germantown, MD 20876 USA.
E-mail: gchen@intfusiontech.com

1. INTRODUCTION

Energy detection is one of the most commonly used approaches for spectrum sensing [1]. The detector operates by comparing the energy of the received waveform over a time window to a threshold determined by the noise floor. An energy detector was first investigated in [2] for the detection of unknown deterministic signals over a band limited additive white Gaussian noise channel. Using the sampling theory, it was shown that the test statistic of the energy detection follows a chi-square distribution under H_0 (no signal transmission) and the non-central chi-square distribution under H_1 (signal transmission exists), based on which the exact false alarm rate and detection probability were derived. In [3,4], the energy is extended for the detection of unknown signals over different types of fading channels. Closed-form expressions for the detection probabilities over Rayleigh, Nakagami, and Rician fading channels were presented. In [5], the optimal sensing time of the secondary user using energy detection is derived to maximize the average throughput and protect the primary user from harmful interference. In [6], performance of two different energy detection methods were compared, where the first (averaging) approach uses the signal power over the whole bandwidth, and the second (maximum) approach detects signal power over individual fast Fourier transform bins.

Conventional methods on energy detections as those mentioned previously assume that the detection tests are independent. However, the assumption only holds when the detection tests use independent data sets from non-overlapping testing windows as in Figure 1(a). As a result, independent tests can only be performed as rate limited by the testing window length. This will cause performance degradation when energy detection is used to monitor a communication channel for the detection of signal

†The views and conclusions contained herein are those of the authors and should not be interpreted as necessarily representing the official policies or endorsements, either expressed or implied, of the Air Force.

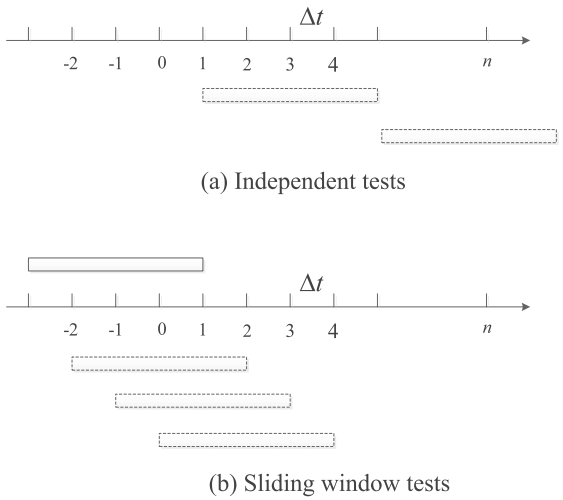

Figure 1. Independent tests versus sliding window tests.

transmission activities. When the window length is large (which is necessary for detection when the signal-to-noise ratio (SNR) at the detectors receiver is low), the independent requirement will significantly increase the detection time and degrade detection speed. Figure 1(b) illustrates the idea of the sliding window test, where tests are performed over every fixed time interval independent to length of the test window.

Testing windows in the sliding window test have overlaps, and as a result, test statistics in the sliding window test are correlated over time. This correlation significantly complicates the design and performance analysis of the sliding window test for spectrum sensing. To address the problem, in this paper, first an effective approximation and a numerical method are proposed for the evaluation of the false alarm of the sliding window energy detection. Interestingly, it is observed that with the same window length and testing threshold, the false alarm rate of a sliding window test and that of the independent test have a relationship that is almost linear. Based on the results, the design of constant false alarm sliding window energy test is addressed. Then using the same approach, detection probabilities of the sliding window test are evaluated for a given window length and an SNR. The corresponding distribution of the detection time is also obtained, which allows the determination of the optimal window length that minimizes the expected detection time. Then simulations are conducted on the sliding window energy detection to show the simulated detection performance versus the theoretical prediction and performance of the conventional energy detection.

The paper is organized as follows. Section 2 briefly reviews conventional energy detection under the independent assumption [2]. For the sliding window test using energy detection, Section 3 presents the algorithms for false alarm analysis and proposes a test design process. The evaluation of the detection probability and the analysis of detection performance are presented in Section 4. Section 5 presents simulation results of the proposed sliding window energy detection. Section 6 summarizes the paper with concluding remarks.

2. INDEPENDENT ENERGY DETECTION TEST REVIEW

First, for readers' convenience, the main notations used in this paper for the description of energy detection are listed as follows, which follow mostly the notations in [3].

$s(t)$	received signal waveform
$n(t)$	noise waveform
N_0	two-sided noise power spectrum density
P_s	signal power
W	one-sided bandwidth in hertz
Δt	sampling interval $=\frac{1}{2W}$
T	testing window length
L	discrete window length $T = L\Delta T$
η	unit time signal-energy-to-noise density ratio (SNR): $\frac{P_s \Delta t}{N_0} = \frac{P_s}{N_0 2W}$
τ	threshold used by energy detector
$N(\mu, \sigma^2)$	Gaussian density with mean μ and standard deviation σ
χ^2_α	Chi-square distribution with degree of freedom α
$\chi^2_\alpha(\beta)$	non-central Chi-square distribution with degree of freedom α and non-centrality parameter β

For energy detection, the received waveform is given by

$$y(t) = \begin{cases} s(t) + n(t) \\ n(t) \end{cases} \tag{1}$$

As shown in [2], for the decision process, the baseband signals and the passband signals are equivalent for the decision process. For the sake of convenience, as in [3], the received signal is assumed to be at the baseband and has a limited bandwidth. According to sampling theory, one can express the noise process as [2]

$$n(t) = \sum_{i=-\infty}^{\infty} n[i]\text{sinc}(2Wt - i) \tag{2}$$

where $\text{sinc}(x) = \frac{\sin(\pi x)}{\pi x}$, and $n[i] = n(\frac{i}{2W}) = n(i\Delta t)$ is a discrete white noise random process with zero mean and variance $2N_0W$, that is,

$$n[i] \sim N(0, 2N_0W) \tag{3}$$

Similarly, for the signal, one has

$$s(t) = \sum_{i=-\infty}^{\infty} s[i]\text{sinc}(2Wt - i) \tag{4}$$

where $s[i] = s(i\Delta t)$. For a test using the data in a time window $[0\ T]$, the test statistic of the energy detection is given by [2]

$$\begin{aligned} V &= \frac{1}{N_0}\int_0^T y(t)^2 dt = \frac{1}{2WN_0}\sum_{i=1}^{2TW} y[i]^2 \\ &= \frac{1}{2WN_0}\sum_{i=1}^{L} y[i]^2 \end{aligned} \tag{5}$$

where

$$L = 2TW \tag{6}$$

is the time-bandwidth product. Assuming $2TW$ is an integer value for the sake of simplicity, then under H_0, one has

$$\frac{y[i]}{\sqrt{2WN_0}} \sim N(0,1) \tag{7}$$

where the symbol "$\sim$" in (7) should be interpreted as "following the distribution of," and

$$V \sim \chi_L^2. \tag{8}$$

Under H_1, one has

$$\frac{y[i]}{\sqrt{2WN_0}} \sim N\left(\frac{s[i]}{\sqrt{2WN_0}}, 1\right) \tag{9}$$

and

$$V \sim \chi_L^2(\lambda) \tag{10}$$

where

$$\begin{aligned} \lambda &= \frac{1}{2WN_0}\sum_{i=1}^{L} s[i]^2 \\ &= \frac{1}{N_0}\int_0^T s(t)^2 dt = \frac{P_s T}{N_0} \end{aligned} \tag{11}$$

is the noncentrality parameter. The probability density function (pdf) of the test statistic is [7,8]

$$f_V(x) = \begin{cases} \frac{1}{2^{L/2}\Gamma(L/2)} x^{L/2-1} e^{-x/2} \\ x \geq 0 \quad , H_0 \\ \frac{1}{2} e^{-(x+\lambda)/2} (\frac{x}{\lambda})^{L/4-1/2} I_{L/2-1}(\sqrt{\lambda x}) \\ x \geq 0 \quad , H_1 \end{cases} \tag{12}$$

where $\Gamma(\cdot)$ denotes the Gamma function and $I_v(z)$ is a modified Bessel function of the first kind. The probability of false alarm (under H_0) and probability of detection (under H_1) are given by [4]

$$P_f = P(V > \tau | H_0) = 1 - \frac{\gamma(L/2, \tau/2)}{\Gamma(L/2)} \tag{13}$$

where $\gamma(k, z)$ is the lower incomplete Gamma function, and

$$P_f = P(V > \tau | H_1) = Q_{\frac{L}{2}}(\sqrt{\lambda}, \sqrt{\tau}) \tag{14}$$

where $Q_M(a, b)$ is the Marcum Q-function [9].

The evaluations of (13) and (14) apply to energy tests that are independent. For the sliding window test, test statistics of multiple tests are correlated and the above evaluations are no longer valid. In Sections 3 and 4, novel algorithms will be developed to address the problem of correlated test statistics.

3. FALSE ALARM EVALUATION FOR SLIDING WINDOW TEST USING ENERGY DETECTION

Suppose the window length of the sliding window energy test is L in discrete time and the tests are conducted at discrete time $[k]$, where $k = 1, 2, 3, \ldots$. The corresponding test statistics are

$$\begin{aligned} V[k] &= \frac{1}{2WN_0}\sum_{i=k-L+1}^{k} y[i]^2 \\ &= \frac{1}{N_0}\int_{(k-L)\Delta t}^{k\Delta t} y(t)^2 dt \end{aligned} \tag{15}$$

Suppose the test starts from $k = 1$, under hypothesis H_0, the sliding window false alarm probabilities, P_{fs}, at the following testing times are

$$P_{fs}[1] = P(V[1] > \tau, H_0) \tag{16}$$

$$P_{fs}[2] = P(V[2] > \tau | V[1] < \tau, H_0) \tag{17}$$

$$P_{fs}[3] = P(V[3] > \tau | V[1] < \tau, V[2] < \tau, H_0) \tag{18}$$

$$P_{fs}[4] = P(V[4] > \tau | V[1] < \tau, V[2] < \tau, V[3] < \tau, H_0) \tag{19}$$

The evaluation of (16) follows directly (13). However, the exact evaluations of (17)–(19) are increasingly more complicated. In this paper, the following approximation is used for the evaluation of false alarm rates in sliding window test

$$P_{fs}[k] = P(V[k] > \tau | V[k-1] < \tau, H_0) = P_{FAs} \tag{20}$$

which is conditioned only on the previous testing result that has the biggest impact on the current test at time k. For the evaluation of (20), Figure 2 shows the relationship between two consecutive test statistics where $V[k-1] = a+b$ is the sum of two independent random variables a and b. Under H_0, one has $a \sim \chi_1^2$ and $b \sim \chi_{L-1}^2$; where $V[k] = b + c$ is the sum of b, which is the common part with $V[k-1]$

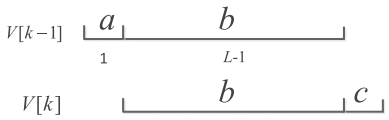

Figure 2. Test statistics of two consecutive tests in the sliding window test.

and random variable c. c follows χ_1^2 and is independent to b and a. To evaluate P_{FAs}, the posterior probability density function of b conditioned on $V[k-1] \leq \tau$, denoted as, $p_b(b|a+b \leq \tau)$, needs to be first evaluated. From Bayes rule, one has

$$p_b(b|a+b<\tau) \propto p_b(b) \int_0^{\tau-b} p_a(a)da \qquad (21)$$

where $p_a(.)$ denotes probability density function (pdf) for a and $p_b(.)$ denotes pdf for b. For the evaluation of (20), it follows

$$\begin{aligned} P_{FAs} &= 1 - P(V[k] \leq \tau | V[k-1] \leq \tau) \\ &= 1 - \int_0^{\tau} \left[p_b(b|a+b \leq \tau) \int_0^{\tau-b} p_c(c)dc \right] db \end{aligned} \qquad (22)$$

The direct evaluation of (21) and (22) is difficult. In this paper, a numerical approach is used. Note that the posterior pdf (21) is non-zero only over interval $[0 \quad \tau]$, which allows the use of a discrete approximation to accurately represent the pdf. To do this, the interval $[0 \quad \tau]$ is evenly divided into N pieces whose probability masses are proportional to the probability density (21) at their center (sampling) points. The discrete approximation of $p_b(b|a+b \leq \tau)$ is obtained as

$$\begin{aligned} &p_b[i|a+b<\tau] \propto \\ &p_b\left(\frac{\tau}{N}\left(i-\frac{1}{2}\right)\right) \int_0^{\frac{\tau}{N}(N-i-\frac{1}{2})} p_a(a)da \\ &i = 1, \ldots, N \end{aligned} \qquad (23)$$

and

$$\sum_{i=1}^{N} p_b[i|a+b<\tau] = 1 \qquad (24)$$

For the evaluation of (22), the following approximation is used

$$\begin{aligned} &\int_0^{\tau} \left[p_b(b|a+b \leq \tau) \int_0^{\tau-b} p_c(c) \right] db \approx \\ &\sum_{i=1}^{N} p_b[i|a+b \leq \tau] \int_0^{\frac{\tau}{N}(N-i-\frac{1}{2})} p_c(c)dc \end{aligned} \qquad (25)$$

Any desired level of evaluation accuracy can be achieved by using sufficiently large N. Figure 3 shows P_{FAs} (22) for the sliding window energy test versus P_f (13) of the independent window test when they use the same window length and the same testing threshold. It can be seen that for the set of window lengths considered $L = 5,\ 50,\ 100,\ 200,$ and 300, P_{FAs} is smaller than P_f by a reduction factor ranging from 1 (no reduction, when the window length is 1) to approximately 0.1 (for long window lengths up to 300), which is due to the correlation of the tests statistics in the sliding window tests. Interestingly, it is observed that for a given window length, P_f versus P_{FAs} (with the same testing threshold) is almost linear, which makes the mapping easy and will greatly simplify the design of a sliding window test.

For the design of the sliding window energy test, we are interested in the cumulative false alarm rate over a long period of K tests, denoted as $P_F(K)$, which is related to P_{FAs} by

$$P_F(K) = 1 - (1 - P_{FAs})^K \qquad (26)$$

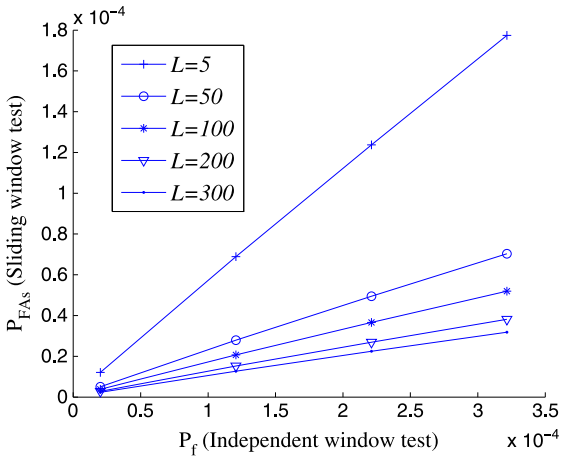

Figure 3. P_{FAs} for the sliding window test versus P_f for independent window test.

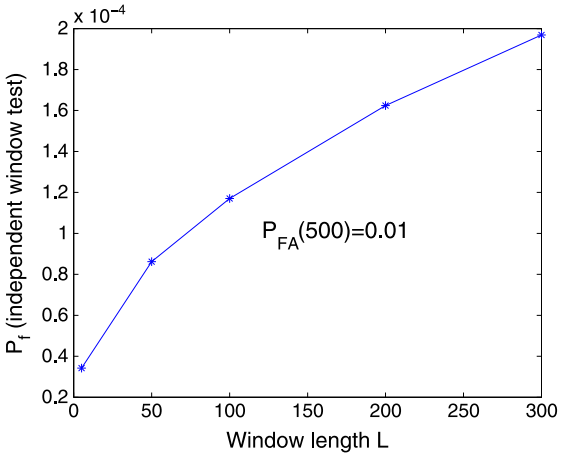

Figure 4. False alarm rates of the corresponding independent window $P_F(500) = 0.01$.

The required false alarm rate for the sliding window test is derived from (26) as

$$P_{FAs} = 1 - (1 - P_F(K))^{1/K} \tag{27}$$

For example, assuming $K = 500$ and $P_F(500) = 0.01$, from (27), one has the required $P_{FAs} = 2.1 \times 10^{-5}$. Based on the mapping between P_f and P_{FAs} for the window lengths of interest (as shown in Figure 3), the corresponding P_f can be evaluated, which from (22) leads to the desired test threshold τ.

Figure 4 shows, when $P_F(500) = 0.01$, the false alarm rates of the independent tests P_f versus the window length L. It can be seen that under the same cumulative false alarm rate requirement for the sliding window tests, a larger window length L allows a higher false alarm rate P_f of the corresponding single independent test.

4. THE EVALUATION OF DETECTION PROBABILITY OF A SLIDING WINDOW TEST USING ENERGY DETECTION AND PERFORMANCE ANALYSIS

Most detection tests in the literature assume that under H_1, the signal always exists in the testing window. In this paper, we investigate a more general case, which allows detection in the presence of transition from H_0 to H_1 and shows the impact of window length on the detection performance. Figure 5 illustrates the detection process when the sliding window length $L = 4$, and without loss of generality, the transition from H_0 to H_1 occurs at 0. The detection probabilities of the sliding window test, P_{ds}, are

$$P_{ds}[1] = P(V[1] > \tau, H_1) \tag{28}$$

$$P_{ds}[2] = P(V[2] > \tau | V[1] < \tau, H_1) \tag{29}$$

$$P_{ds}[3] = P(V[3] > \tau | V[1] < \tau, V[2] < \tau, H_1) \tag{30}$$

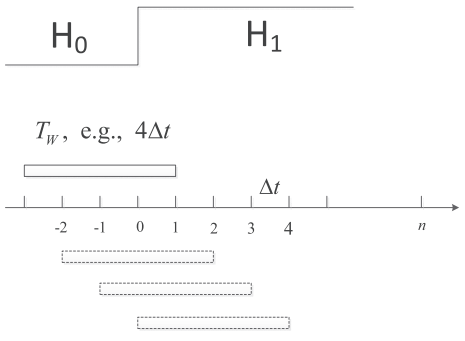

Figure 5. An illustration of the detection process of the sliding window test.

where the test statistics $V[k]$ are given by (15) and the testing threshold τ is determined based on the requirement on the cumulative false alarm rate for the sliding window test (26) using the design procedure proposed in Section 3. As the case of the false alarm evaluation, the exact evaluations of these detection probabilities are very complicated especially for long window lengths. Instead, the same approximation proposed in Section 3 is used for the evaluation of sliding window detection probabilities, that is,

$$P_{ds}[k] = P(V[k] > \tau | V[k-1] < \tau, H_1) = P_{Decs} \tag{31}$$

The same approach for the evaluation of false alarm of the sliding window test can be used for the evaluation of the detection probabilities. The two consecutive test statistics under H_1 bear the same relationship as illustrated in Figure 2. Similar to 21, one has

$$\begin{aligned} P_{Decs} &= 1 - P(V[k] \le \tau | V[k-1] \le \tau, H_1) \\ &= 1 - \int_0^{\tau} \left[p_b(b | a + b \le \tau) \int_0^{\tau - b} p_c(c) dc \right] db \end{aligned} \tag{32}$$

But under H_1, the posterior density $p_b(b|a + b \le \tau)$ is evaluated under the condition that

$$a \sim \chi_1^2(h\eta), \quad h = 0, 1 \tag{33}$$

where h is 0 when at $k - 1$, there is no signal exists in the first Δt portion of the testing window, otherwise $h = 1$, and

$$\eta = \frac{P_s \Delta t}{N_0} = \frac{P_s}{N_0 2W} \tag{34}$$

is defined as the unit time signal-energy-to-noise density ratio, namely, the SNR. For the common part b of $V[k-1]$ and $V[k]$ (Figure 2), one has

$$b \sim \chi_{L-1}^2(m\eta), \quad m = 1, \ldots, L-1 \tag{35}$$

where m is determined by the number of Δt when the signal exists in the b portion of the testing window. And under H_1, c follows $\chi_1^2(\eta)$. To evaluate (32), the same numerical approach as in (25) is used.

Assuming the switch from H_0 to H_1 occurred at time 0, Figure 6 shows the detection probabilities of a sliding window test for a set of window lengths ($L = 5, 50, 100, 200, 300$) from discrete testing times 1 to 400. When the unit time signal noise ratio (34), that is, SNR, is 0.4, then the required cumulative false alarm rate $P_F(500) = 0.01$. It can be seen that for a given window length, after the switching from H_0 to H_1, the detection probabilities increase as the signal containing portion of the testing window increases. The detection probability reaches its peak when the signal portion fills the whole window length. As the window length increases, the peak

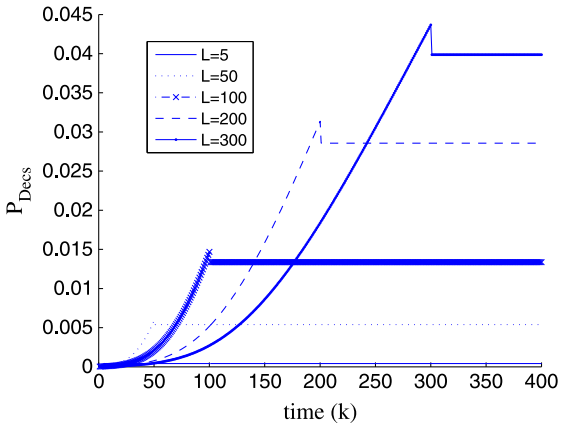

Figure 6. Detection probabilities of sliding window test P_{Decs} versus time when and $P_F(500) = 0.01$.

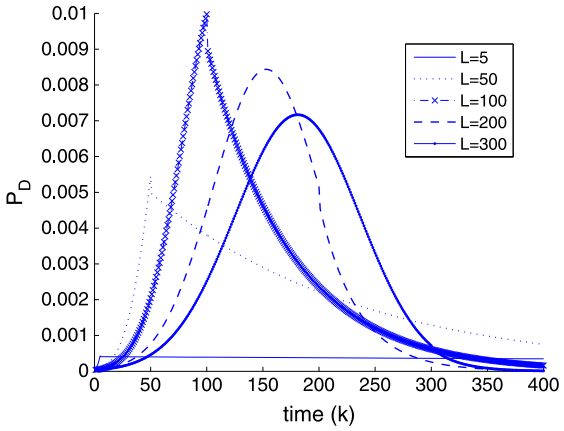

Figure 7. Probability mass function of detection time for the set of window lengths when $\eta = 0.4$ and $P_F(500) = 0.01$.

detection probability of the sliding window test increases; however, the rate of the increase in detection probability decreases. After reaching the peak detection probability, the detection probabilities of the following tests drop a certain amount due to correlations between the consecutive tests. It can be seen that different window lengths have different trade-offs between the speed of the detection and the achievable detection probability.

Figure 7 shows the distributions of detection time for the set of window lengths considered over a time period of 400 testing times. The probability mass function of detection time is obtained from P_{Decs} (32) by

$$P_D(k) = \prod_{i=1}^{k-1}(1 - P_{Decs}(i))P_{Decs}(k) \qquad (36)$$

For window lengths ranging from 20 to 300, Figure 8 shows the cumulative probabilities of detection at the end of the testing period 400; Figure 9 shows their expected

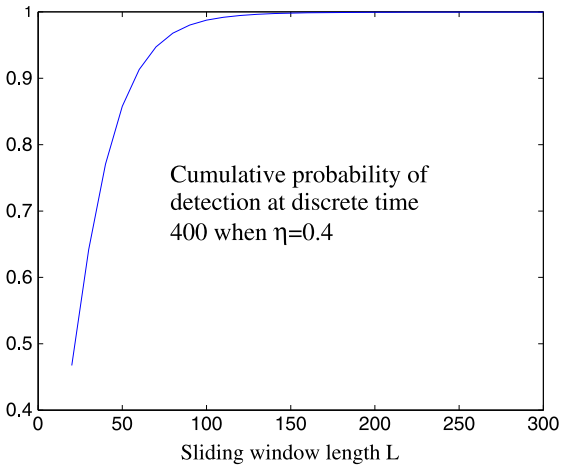

Figure 8. Cumulative probability of detection at time 400 when $\eta = 0.4$ and $P_F(500) = 0.01$.

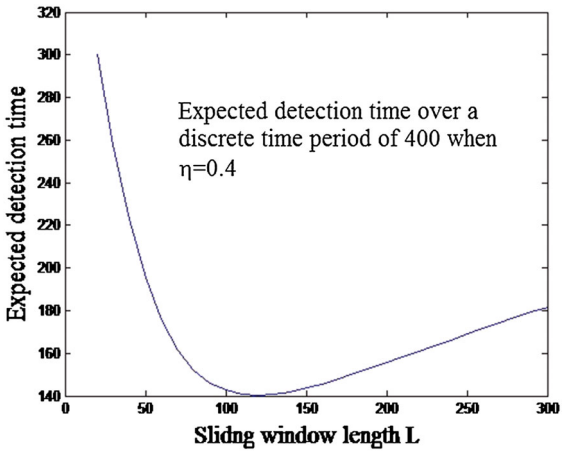

Figure 9. Expected detection time when $\eta = 0.4$ and $P_F(500) = 0.01$.

detection time. Note that when there is no detection during the testing, which occurs quite often with small window lengths (as indicated in Figure 9) the detection time is counted as 400. It can be seen that for the given unit time SNR ratio, the expected time versus the sliding window length takes a convex curve. When $\eta = 0.4$ and $P_F(500) = 0.01$, the optimal window length for the sliding window energy detection minimizes the expected detection time, is for $L = 120$. Similar detection performance analysis of the sliding window tests can be conducted for different unit time signal-energy-to-noise-density ratio, that is, SNR, levels. The performance analysis of the sliding window energy detection is conducted assuming the detector side unit time SNR density ratio η is known. In practice, when η is not known exactly, the analysis needs to be conducted over the range of η values of interest for the selection of an appropriate testing window length.

5. SIMULATION RESULTS

In this section, we first compare the simulated sliding window detection performance to the theoretical performance evaluation of the sliding window energy detection based on the derivation in Sections 3 and 4. Then comparison between the sliding window energy detection and conventional energy detection will be presented to show the advantage of the sliding window energy detection for continuous channel monitoring.

5.1. Simulated performance versus theoretical performance of the sliding window test

The simulation for sliding window energy detection is configured as follows. Without loss of generality, it was assumed that the sliding window test is conducted through discrete time 1 to discrete time N, for a total of N tests. The actual simulation data were generated form discrete time $-L$ to N, where L is the length of the sliding window.

Under H_0, at each sample time, the sample data were generated from $N(0,1)$ based on (7). Under H_1, it is assumed that the signal arrived at the detector at discrete time 1, and starting form time 1, the sample data were drawn from $N(\sqrt{\eta},1)$ based on (9)–(11) and (34); for $-L$ to 0, the sample data were drawn from $N(0,1)$.

Figure 10 shows the data from one simulation run, when $N = 500$, $L = 200$, and $\eta = 1$. Here, the value of η, the SNR, was chosen for illustration purposes only. Actual η used in the simulation is smaller, which makes the data under H_0 and H_1 hard to distinguish.

For the first case, the sliding window detector has length $L = 200$ and was designed to have $P(300) = 0.01$ (26), simulation time $N = 500$ and the signal energy per sample time-to-noise density ratio $\eta = 0.5$.

Under H_0, the simulated cumulative false alarm rate over 300 tests is $\bar{P}(300) = 0.0067$, which is an average over 10,000 simulation runs. This is smaller than the designed cumulative false alarm rate of 0.01 because of the approximation used in (20), which tends to give a conservative (larger) approximation of actual false alarm rate evaluation at single testing times (17)–(19). However, this conservative design always guarantees the cumulative false alarm rate requirement to be met.

Under H_1, Figure 11 shows the simulated probability mass function (pmf) of the detection time (from 10,000 simulations) compared with the theoretical prediction using the method in Section 4. It can be seen that the theoretical prediction characterizes well the trend of simulated distribution. The cumulative probability of detection over the $N = 500$ tests is 0.9976, while the theoretically predicted probability of detection over $N = 500$ tests is 1. The theoretical prediction on detection probability

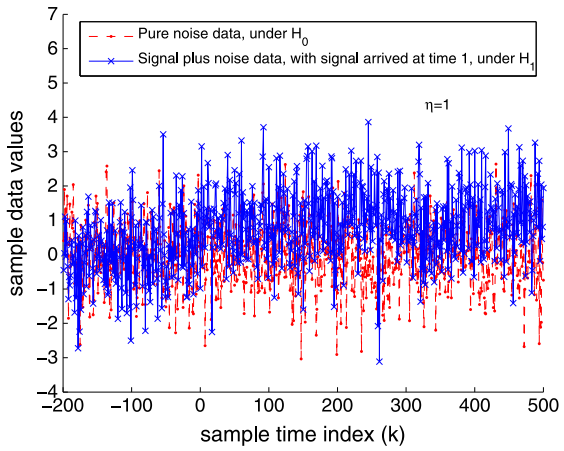

Figure 10. Exemplar simulation data $\eta = 1$ and $N = 500$.

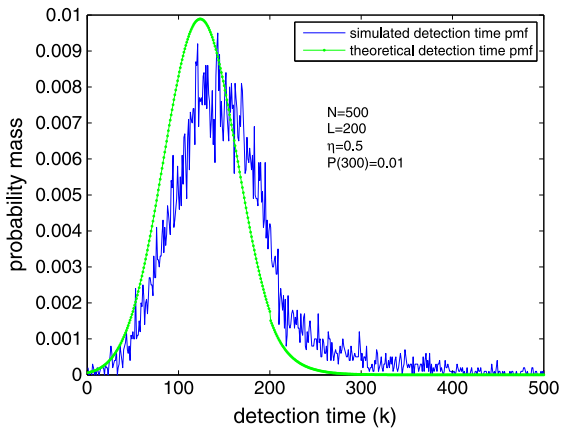

Figure 11. Simulated versus theoretically predicted probability mass function (pmf) of the detection time for $L = 200$, $P(300) = 0.01$, $N = 500$, and $\eta = 0.5$.

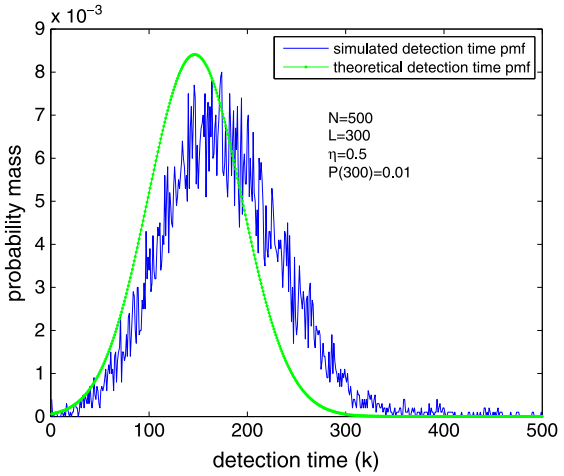

Figure 12. Simulated versus theoretically predicted probability mass function (pmf) of the detection time for $L = 200$, $P(300) = 0.01$, $N = 500$, and $\eta = 0.5$.

is slightly optimistic (higher) than the actual simulated results. Similar to the false alarm case, this is caused by the approximation in (31) for evaluating the single time probability of detection of the sliding window test (29) and (30), which results in evaluations slightly larger than their actual values. The predicted average detection time is 125.2, while the simulated detection time is 153.5, which corresponds to a 22% increase. This is again explained by the larger than actual theoretical prediction of the single time detection probability, which makes the predicted pmf shift towards smaller detection times.

In the second case, we increased the window length to $L = 300$, and the rest of the simulation configuration remained the same. Under H_0, the simulated cumulative false alarm rate over 300 tests is $\bar{P}(300) = 0.0062$, a similar value as in the first case.

Figure 12 shows the pmf of the detection time of the sliding window energy detector. The simulated cumulative detection probability over 500 tests is 1, which is the same as the theoretical prediction. The simulated average detection time is 178.6, and the theoretical prediction is 147.3. Similarly, the actual detection time has a 21% increase over the theoretically predicted value, because of the slightly biased (larger than actual value) approximation of single time test detection probability using (31).

5.2. Sliding window energy detection versus conventional energy detection

In this section, performance of the proposed sliding window energy detection is compared with that of the conventional energy detection. Suppose window length of the conventional energy detection is equal to K as in the specification of the cumulative false alarm rate in (26), and the false alarm rate of the energy detection is set as $P(K)$. Using the scenario specified in Section 5.1, the conventional energy detection is applied only once at time K, which uses data from time 1 to K. Note that although the sliding window energy detection is more complex to design than the conventional energy detection, they have the same level of implementation complexity because both detection algorithms involve mainly the integration of signal energy over time (5).

When $K = 300$ and $P(K) = 0.01$, it is easy to obtain that the conventional energy detection uses a testing threshold of 359.9 and has a detection probability of 0.997.

While the sliding window energy detection with $L = 300$ uses a testing threshold of 389.6 and has a simulated cumulative detection probability of 0.973 over time period if 1 to K. The average detection time for the sliding window detection is 171.8 over the same time period.

For sliding window energy detection with $L = 200$, the cumulative detection probability over time 1 to K is 0.9609, while the average detection time over the same time period is 146.1.

Comparing the detection performance during time 1 to K, the conventional energy detection has the highest detection probability and the largest detection time K. The sliding window tests has reduced detection power but significantly reduced detection time. And it is worth pointing out that in this comparison, the conventional energy detection has the unfair advantage of knowing the starting time of the signal. If the conventional energy detection test is conducted at a time point less than K, its detection power would be significantly reduced.

From the previously mentioned comparison, it can be seen that the sliding window energy detection is suitable for constantly monitoring a spectrum channel for fast detection of signal presence under low SNR scenarios, where effective signal detection is only possible with large time-bandwidth product (6).[†] While the conventional energy detection is used to check occasionally if signal is prepense over a channel.

6. CONCLUSIONS

The paper investigates performance of the energy detection when used in a sliding window fashion for monitoring signal transmission activities in a frequency band. Unlike conventional independent energy tests, test statistics in the sliding window test are correlated over time, which complicates the design of the test and the evaluation of the testing performance. In this paper, for the design of the sliding window energy detection, algorithms are proposed to effectively evaluate the false alarm rate and the detection probability of the proposed detection algorithm. It is observed that, with the same window length and testing threshold, the false alarm rate of the sliding window energy test and that of the independent test have a relationship that is almost linear, which is further utilized to simplify the false alarm evaluation. Then the distribution of the detection time is obtained for given window length and SNR, which allows the evaluation of the impact of window length on the performance of the sliding window test.

Based on the proposed design, simulations of the sliding window energy detection were conducted. It was shown that the theoretical prediction of the sliding window energy detection performance characterizes well the trend of simulated distribution of the detection time. While a small bias does exist in the theoretical evaluation because of the approximation used the evaluation procedure. Performance of the sliding window energy detection was then compared with that of the conventional energy detection. It was shown that the sliding window energy detection offers faster detection speed, which makes it suitable for continuous monitoring of spectrum channels for the detection of a signal in low SNR conditions.

[†]In high SNR detection scenario, the speed advantage of the sliding window detection is negligible due to overall short detection time.

ACKNOWLEDGEMENT

This work was supported in part by the United States Air Force under contracts FA9453-11-1-0290 and FA9453-12-M-0022.

REFERENCES

1. Yucek T, Arslan H. A survey of spectrum sensing algorithms for cognitive radio applications. *IEEE Communication Surveys & Tutorial* 2009; **11**(1): 116–130.
2. Urkowitz H. Energy detection of unknown deterministic signals. In *Proceedings of the IEEE*, April 1967; 523–531.
3. Digham FF, Alouini MS, Simon MK. On the energy detection of unknown signals over fading channels. In *IEEE International Conference on Communications*, Anchorage, Alaska, 2003; 3575–3579.
4. Kostylev VI. Energy, detection of a signal with random amplitude. In *Proceedings of the IEEE International Conference on Communications*, NYC, New York, 2002; 1606–1610.
5. Ghasemi A, Sousa ES. Optimization of spectrum sensing for opportunistic spectrum access in cognitive radio networks. In *Proceedings of the 4th IEEE Consumer Communications and Networking Conference*, Las Vegas, NV, 2007; 1022–1026.
6. Boksiner J, Dehnie S. Comparison of energy detection using averaging and maximum values detection for dynamic spectrum access. In *Proceedings of the 34th IEEE Sarnoff Symposium*, Princeton, NJ, USA, 2011; 1–6.
7. Chi-squared_distribution: http://en.wikipedia.org/wiki/Chi-squared_distribution.
8. Noncentral_chi-squared_distribution: http://en.wikipedia.org/wiki/Noncentral_chi-squared_distribution.
9. Gezici S, Sahinoglu Z, Poor HV. On the optimality of equal gain combining for energy detection of unknown signals. *IEEE Communications Letters* 2006; **10**(11): 772–774.

AUTHORS' BIOGRAPHIES

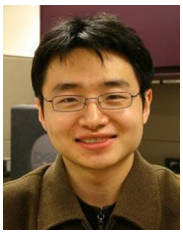

Xin Tian received the BS and MS degrees in communication systems from the Department of Information and Communication Engineering, Xi'an Jiaotong University, China, in 2002 and 2005. In 2010, he received the PhD degree in electrical engineering from the Department of Electrical and Computer Engineering, University of Connecticut, Storrs, CT, USA. He currently works as a senior research scientist at Intelligent Fusion Technology, Inc., Germantown MD, USA. His research interests include statistical signal processing, tracking algorithms, information fusion, sensor resource management, and communication systems.

Zhi Tian is a professor in the Electrical and Computer Engineering Department of George Mason University, Fairfax, VA, USA, as of January 2015. Prior to that, she was on the faculty of Michigan Technological University from 2000 to 2014. Her research interests lie in statistical signal processing, wireless communications and wireless sensor networks. She is an IEEE Fellow. She is an elected member of the IEEE Signal Processing for Communications and Networking Technical Committee and a member of the Big Data Special Interest Group IEEE Signal Processing Society. She served as Associate Editor for *IEEE Transactions on Wireless Communications* and *IEEE Transactions on Signal Processing*. She is a Distinguished Lecturer of the IEEE Vehicular Technology Society from 2013 to 2017 and the IEEE Communications Society from 2015 to 2016.

Erik Blasch received his BS in Mechanical Engineering from the Massachusetts Institute of Technology (1992) and PhD in Electrical Engineering from Wright State University (1999) in addition to numerous master's degrees in mechanical engineering, industrial engineering, electrical engineering, medicine, military studies, economics, and business. He has been with the Air Force Research Laboratory since 1996 compiling over 500 papers. He is a Fellow of SPIE, Associate Fellow of AIAA, and a senior member of IEEE. His areas of research include target tracking, image fusion, information fusion performance evaluation, and human-machine integration.

Khanh Pham serves as a senior aerospace engineer with the Air Force Research Laboratory-Space Vehicles Directorate. He is a senior member of IEEE, SPIE, and an associate fellow of AIAA. His BS and MS degrees in electrical engineering are from the University of Nebraska and PhD in electrical engineering from the University of Notre Dame. His research interests include statistical optimal control and estimation; fault-tolerant control; dynamic game decision optimization; security of cyber-physical systems; satellite cognitive radios; and control and coordination of large-scale dynamical systems.

Dan Shen received his MS and PhD degrees in electrical and computer engineering from Ohio State University in 2003 and 2006. He then worked as a research scientist at Intelligent Automation Inc. (MD) and as a project manager at DCM Research Resources LLC (MD). He is currently a principal scientist at IFT, where his interests include game theory and its applications, optimal control, and adaptive control.

Genshe Chen received the BS and MS degrees in electrical engineering, PhD in aerospace engineering, in 1989, 1991 and 1994, respectively, all from Northwestern Polytechnical University, Xian, China. Currently, Dr. Chen is the Chief Technological Officer of Intelligent Fusion Technology, Inc., Germantown, MD. His research interests include satellite communication, cooperative control and optimization for military operations, target tracking and multisensor fusion, cyber security, C4ISR, electronic warfare, digital signal processing and image processing, game theoretic estimation and control, and human-cyber-physical system.